Improved YOLOv8 Real-Time Detection Algorithm for Surface Defect in Drug Aluminum-Plastic Blister

Baomin Wang, Zhirong Wang, Wang Wang, Liangjun He, and Hongqin Liu

Abstract—**Due to machine instability and other uncontrollable factors, defects and damage may occur in the aluminum-plastic blister packs during the drug packaging process. Several challenges have restricted the traditional defect detection methods, such as low accuracy and high costs, which makes the traditional methods inadequate for efficient and precise detection. To address these issues, this paper proposed an optimized deep learning defect detection model based on the YOLOv8 network, which aimed at the enhancement of detection performance and robustness. Firstly, Weighted Bidirectional Feature Pyramid Network (BiFPN) was integrated into the YOLOv8 to enhance the detection performance of small defects, thus improving the overall effectiveness of the model. Meanwhile, Group-Shuffle Convolution (GS-Conv) was employed to replace the conventional convolutional layers, which could enable efficient extraction of defective features and reduce the model complexity. Moreover, the GIOU loss function was introduced in place of the original loss function, which could improve the accuracy of the prediction box and the convergence speed of the model. According to the results, it was demonstrated that the proposed model achieved an accuracy of 89.5% and an mAP@0.5 of 82.4% on a self-constructed aluminum-plastic blister defect dataset. These improvements provide a valuable reference for the identification and detection of defects in drug blister packaging, contributing to the advancement of intelligent quality control in drug manufacturing.**

Index Terms—**Drug aluminum blister, Surface defect, Detection algorithm, YOLOv8, Deep learning**

I. INTRODUCTION

IN the process of drug production and packaging, there are many defects caused by various uncontrollable factors, such as missing particles, powder leaking, aluminum-plastic blister bending, poor sealing, and excessive cutting of aluminum foil [1]. Therefore, drug defect detection exhibits crucial functions in the practical production [2]. Notably, traditional detection methods are predominantly dependent on manual selection of defective products, which is inefficient, costly, and prone to errors [3]. With the development of technologies in the past few decades, detection methods have evolved from initial visual observation to radiographic inspection [4], ultrasonic testing [5], magnetic particle testing [6], and eddy current testing [7]. Additionally, deep learning technology has been widely applied in defect detection with the rapid advancement in computer technology.

For product defect detection, many studies have been done on deep learning technology [8,9]. Wang et al. [10] designed a network traffic anomaly detection method based on the DGBi-SA model, through a series of experiments, the results showed that AUC, accuracy, recall, and F1 score were superior to other methods. Liao et al. [11] explored a new helmet detection algorithm PSP-RTMDet based on real-time object detectors, and compared with the YOLOv8 algorithm, the detection accuracy has been significantly improved. Hou et al. [12] developed a lightweight remote sensing image object detection algorithm based on YOLOv9, tested on the SIMD dataset, the approach significantly reduces model parameters and GFLOPs, and achieving improvement in detection accuracy. Girshick et al. [13] proposed a simple and scalable detection algorithm, the approach combines region proposals with CNNs, and the mean average precision (mAP) has been greatly improved. Ren et al. [14] introduced a Region Proposal Network (RPN) that shares full-image convolutional features with the detection network, and merged RPN and Fast R-CNN into a single network by sharing their convolutional features, the results showed this method improved object detection accuracy. He et al. [15] extended Faster R-CNN to predict an object mask by adding a branch in parallel with the existing branch for bounding box recognition. Hao et al. [16] designed an intelligent industrial inspection method for steel surface defects, and this method showed high efficiency in inference. Ma et al. [17] improved a YOLO-MF model based on YOLOv3 for pavement crack detection, and the F1 score is higher. Wang et al. [18] put forward an improved YOLOv7 detection method for steel surface defects, it has higher performance. Li et al. [19] integrated SE attention mechanisms and introduced BiFPN in YOLOv5, this method has high recognition accuracy, fast detection speed, and small memory occupation. CAO et al. [20] improved YOLOv8-GD model for defect detection in electroluminescence images of solar photovoltaic modules, and achieved high mAP, moreover its size is small. Liu et al. [21] enhanced the YOLOv8 model for surface damage detection of wind

Manuscript received February 25, 2025; revised July 11, 2025.
This work was supported in part by the National Natural Science Foundation of China (Grant No. 51965038).
Baomin Wang is a professor in the School of Electrical and Mechanical Engineering, Lanzhou University of Technology, Lanzhou 730050, P. R. China (corresponding author to provide phone: +86-138-9349-1613; e-mail: wbm2007@163.com).
Zhirong Wang is a graduate student in the School Lanzhou University of Technology, Lanzhou 730050, P. R. China (e-mail: w543693453@163.com).
Wang Wang is a graduate student in the School Lanzhou University of Technology, Lanzhou 730050, P. R. China (e-mail: 1872428994@qq.com).
Liangjun He is a graduate student in the School Lanzhou University of Technology, Lanzhou 730050, P. R. China (e-mail: 18393134112@163.com).
Hongqin Liu is a lecturer in the School of Electrical and Mechanical Engineering, Lanzhou University of Technology, Lanzhou 730050, P. R. China (e-mail: liuhongqin2005@163.com).

turbines, and improved average precision. Fang et al. [22] used SURF algorithm to extract features of the tested drug, and classified the tested drug using BOW model and SVM, which improved the accuracy and stability of defect detection. Vijayakumar et al. [23] optimized a CBS-YOLOv8 detection model by adding Weighted Bidirectional Feature Pyramid to detect the quality of tablets in blister package. Ma et al. [24] presented a lightweight YOLOv8 model, using for real-time detection of multi-stage apple fruit in complex orchard environments, and improved detection speed. Chen et al. [25] constructed a portable real-time damage detection system for concrete bridge based on YOLOv8, and improved the detection accuracy.

As mentioned above, although deep learning-based defect detection algorithms have been successfully applied in industrial production, the relevant studies on the defect detection of drug aluminum-plastic blisters are relatively lacking. Based on the above finding, the main contributions of this study are as follows: (1) Introducing Weighted Bidirectional Feature Pyramid Network (BiFPN) to capture the detailed information of small targets, which improved the performance and robustness of the model. (2) Adopting the Group-Shuffle Convolution (GS-Conv) network to reduce the complexity of the model, alongside the effective extraction of features. (3) Applying the loss function GIOU in the YOLOv8 algorithm to improve the accuracy of prediction boxes, alongside the enhancement of the convergence speed of the model.

II. Network Models

A. YOLOv8 Basic Network Model

As a deep learning algorithm for real-time target detection, the YOLO (You Only Look Once) algorithm was first proposed in 2016 by Joseph Redmon et al. [26]. Which aimed at a single forward pass of a neural network for target localization and classification. Based on the outstanding advantages in efficiency and speed, YOLOv8 exhibits excellent performance in practical applications, and it has become one of the most advanced detection algorithms available.

YOLOv8 is the latest version of the YOLO series, which is characterized by higher accuracy, smaller size, and faster speed. Specifically, it has five models, which are composed of YOLOv8n, YOLOv8s, YOLOv8m, YOLOv8l and YOLOv8x. These five models are sequentially arranged with the increase of network depth and width, and the design concept is the quickly and accurate detection of the targets through the efficient network structure in different scenarios. As an advanced detection model, YOLOv8 is a cross-stage target detection model following the YOLOv5 series, which could enhance the performance, flexibility, and efficiency based on the incorporation of new features.

The YOLOv8 model is composed of four main parts, including input, backbone, neck, and head. The visual detection tasks are mainly composed of detection, segmentation, pose estimation, and classification. The specific network structure is shown in Fig. 1. The principle of the method is to normalize the input image and extract the main features of the image by the backbone network after adjusting to the required fixed size. Subsequently, the neck network is used to fuse the features of the image at different scales. Finally, the fused image feature is processed to generate the final prediction results based on the detection head.

B. YOLOv8-BGG defect detection algorithm

Introduction of Weighted Bidirectional Feature Pyramid Networks

As a neural network structure BiFPN could be used in target detection and instance segmentation, and it is based on the traditional Feature Pyramid Network (FPN), and its structure is shown in Fig. 2. Functionally, BiFPN has two branches, from the top-down and from the bottom-up. Unlike FPN, BiFPN establishes a connection between

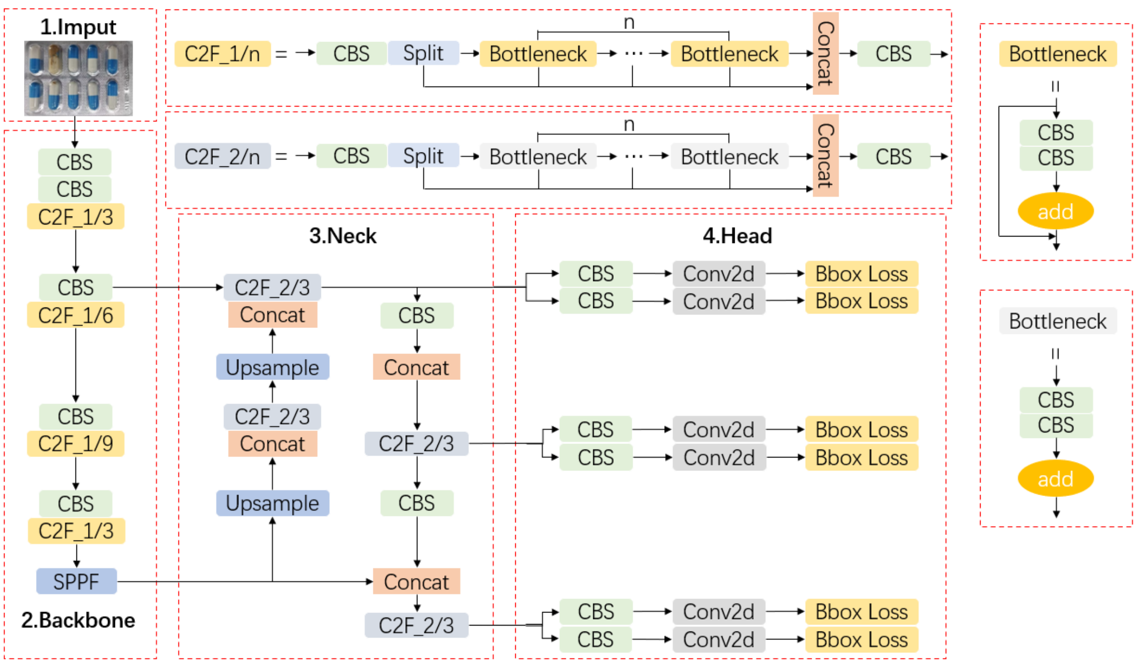

Fig. 1 The Network Structure of YOLOv8

the two branches, which contributes to the more effective fusion of information between features of different scales. Compared to the feature fusion networks in YOLOv8, BiFPN alleviates the influence of single-scale feature nodes with minimal contribution, alongside the emphasis of multi-scale fusion nodes. During the process of feature fusion, instead of the simple combination of features, BiFPN optimizes the fusion results based on the adjustment of weights and selection of dynamic characteristics, which contributes to the effective utilization of the important features of the detected target.

Moreover, direct jump connections are added between the input and output nodes by BiFPN, and the feature information can be extracted around the target by various types of branches and jump connections. Consequently, BiFPN enhances the efficiency and effectiveness of feature fusion based on a simplified bidirectional network structure, additional edges, and repeated bidirectional paths, which could effectively overcome the limitations of traditional FPN.

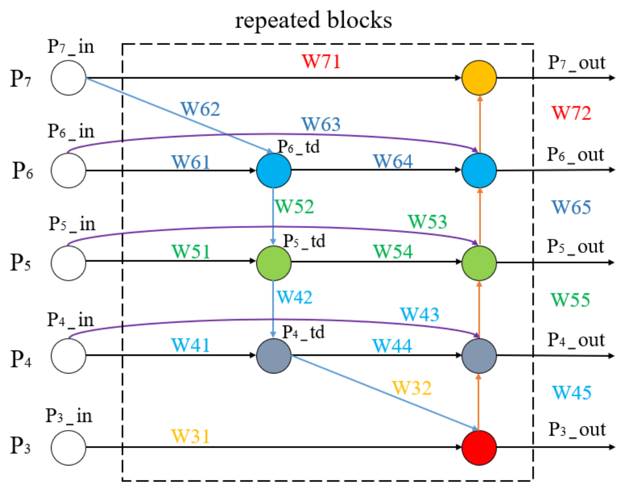

Fig. 2 BiFPN Structure

Improvement of Convolutional Networks

In this study, Group-Shuffle Convolution (GS-Conv) is employed instead of traditional convolutional networks, and its structure is shown in Fig. 3. As a variant of convolutional networks, GS-Conv can improve computational efficiency in convolutional neural networks. In the CNN structure, the images need to be gradually transferred from spatial feature information to channel information, during which the size of the input image must be compressed, which may result in the loss of defective features. Therefore, the computational effort will be greatly increased to minimize the loss of defective features. GS-Conv first performs group convolution, followed by mixing the channels of the feature map through a mixing operation, which can maintain the characterization ability of the network structure while reducing the cost of computation. Therefore, GS-Conv serves as one of the key technologies in lightweight network design, which could enable more effective feature extraction and representation of the network with smaller model sizes and lower computational effort.

Optimization of loss function

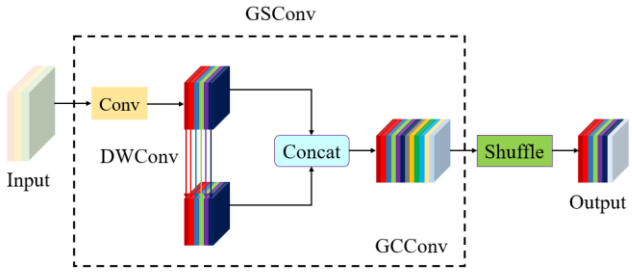

Fig. 3 GS-Conv Structure

The detection performance of the model exhibits a strong connection with the loss function, and the bounding box regression loss function DFL + CIOU Loss is applied in the YOLOv8 model. Specifically, CIOU Loss combines the intersection to union ratio calculation, the distance between two bounding box centroids, and the aspect ratio. Additionally, it could minimize the overlap area between the predicted box and the real box, the distance between center points, and the aspect ratio, which could solve the problem that the IOU function cannot reflect the distance between the predicted box and the real box under the condition that the two factors have no intersection. However, the IOU function fails to effectively deal with the imbalance between difficult and easy samples, and it is insensitive to small targets and the distance between the centroids. Notably, the CIOU function exhibits several disadvantages, such as high computational complexity, increased parameters, and difficulty in training. In view of this, the GIOU loss function is traduced in this study, which takes into account the overlapping and non-overlapping regions between the predicted box and real box, alongside the minimum closure region of their bounding box size.

The GIOU is calculated as follows

$$L_{GIOU} = 1 - IOU - \frac{C-U}{C} \tag{1}$$

where, IOU represents the ratio of the intersection and union of the prediction box and the real box.C represents the minimum closure region between the real box and the prediction box. U represents the concatenation region of the prediction box and the real box. And the value range of GLOU is [-1,1], when the prediction box and the real box overlap, it takes the maximum value of 1. When the prediction box and the real box have no intersection and infinitely far away, it takes the minimum value of -1.

III. Experimental Data And Evaluation Indicators

A. Experimental environment

The working environment is mainly composed of hosting system for Dell Precision 3650 tower workstation, NVIDIA GeForce RTX 3060 graphics card, and memory is 64-bit Windows 10 operating system. The processor is the Intel Core i5-12500, with a main frequency of 3.0GHz and a memory of 32GB. Besides, the computation is accelerated by GPU and the development platform is PyCharm. Additionally, the framework for the network model is based on the PyTorch framework with the application of Python 3.8 and PyTorch 1.11.0 versions, while YOLOv8n is determined as the basic detection model.

B. Dataset preparation

Aluminum-plastic blister defect types can be basically divided into two categories, aluminum-plastic blister defects and drug defects. Specifically, the common defects of aluminum-plastic blisters are aluminum-plastic plate bending (PB), aluminum-plastic film cutting too long (CL), and poor sealing (PS), while the drug defects are missing drugs (MD), and broken drugs (BD). Therefore, effective methods are necessary for the detection and classification of defective aluminum-plastic blisters [27]. The required dataset samples for this experiment are obtained after the processing, and there are five typical defect samples in this dataset, as shown in Fig. 4. The construction of a dataset of surface defects is crucial for the detection of defects in aluminum-plastic blisters. The dataset was initially enhanced to increase the amount of data, followed by the adjustment of its resolution to the size required for the YOLO model (640 × 640 pixels) by a resolution processor, and a total of 2,416 images were obtained.

The processed dataset is labeled by Labeling software, in which the labeling method is the application of a rectangular box to label the defects, and five defect types are obtained during the labeling process, including 'PB', 'CL', 'PS', 'MD' and 'BD'. Subsequently, an XML folder is generated with the same name as the image after the completion of the annotation, and the file includes the annotation information for each image. Whereafter, the resulting images and image XML files are divided into training set, validation set and testing set in the ratio of 8:1:1 by a specific Python code.

C. Model evaluation

In the process of defect detection, relying solely on the accuracy of detection results as an evaluation indicator is not sufficient. So, some evaluation indicators are needed to qualitatively analyze the model detection results. Precision (P), Recall (R), and mean Average Precision (mAP) were adopted, as shown in Eqs. (2)–(5):

$$P = \frac{TP}{TP + FP} \tag{2}$$

$$R = \frac{TP}{TP + FN} \tag{3}$$

$$AP = \int_0^1 P(R)dr \tag{4}$$

$$mAP = \frac{\sum_{i=1}^{k} AP_i}{k} \tag{5}$$

where, TP represents the number of correctly detected boxes for drug defects, FP represents the number of incorrect bounding boxes, FN represents the number of undetected boxes for drug defects, AP_i represents the AP value for class i. k is the number of categories of model target detection, in this study, there are five categories of detection objects, so k =5.

IV. Experimental Results And Discussion

A. Ablation experiments

The objective of the ablation experiments is to illustrate the importance of each improvement in the proposed model. Therefore, BiFPN, GS Conv, and loss function GIOU were added based on YOLOv8n, respectively. The five comparative models mentioned above are trained and tested individually to obtain the comparison results of their complexity and performance, and the experimental results are shown in TABLE I.

TABLE I
ABLATION EXPERIMENTS

model	P	R	mAP@0.5
YOLOv8n	0.865	0.747	0.791
YOLOv8n+BiFPN	0.870	0.742	0.801
YOLOv8n+GS-Conv	0.878	0.752	0.793
YOLOv8n+GIOU	0.890	0.748	0.807
YOLOv8n+BGG	0.895	0.771	0.824

Compared to the original model, it could be found that although the recall is decreased by 0.5% with the addition of BiFPN, but the precision and mAP@0.5 are increased by 0.5% and 1%. Therefore, the model exhibits better feature fusion with the introduction of BiFPN. When replacing the traditional convolutional network with the GS-Conv, the precision has improved by 1.3%, the recall has increased by 0.5%, and mAP@0.5 has increased by 0.2%. Therefore, Group-Shuffle convolutional network could reduce the cost of computation and improve the speed of training, while making the network structure lightweight and maintaining the characterization ability of the network structure. With the

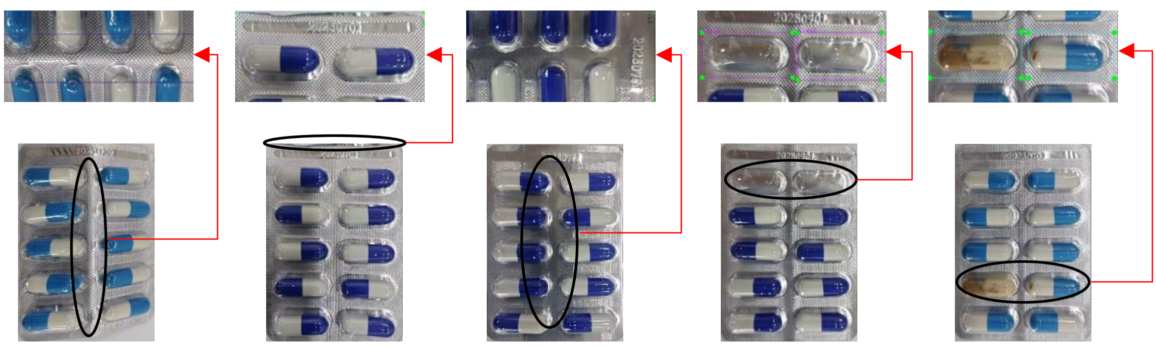

(a) PB (b) CL (c) PS (d) MD (e)BD

Fig. 4 Sample of defect type of aluminum-plastic blister

TABLE II
COMPARISON EXPERIMENT

model	P	R	mAP@0.5
Faster R-CNN	0.801	0.674	0.702
SSD	0.795	0.659	0.677
YOLOv5	0.827	0.698	0.710
YOLOv8	0.865	0.747	0.791
Improved YOLOv8	0.895	0.771	0.824

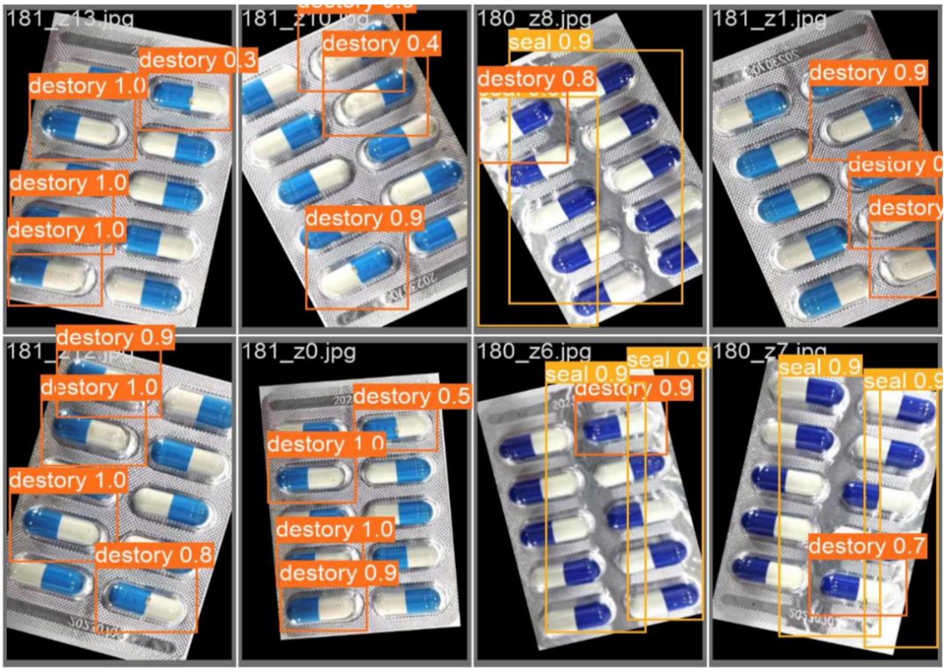

(a)

(b)

Fig. 5 Results Comparison

application of the loss function of GIOU, the precision of the optimized model is improved by 2.5%, the recall is improved by 0.1%, and mAP@0.5 has increased by 1.6%. It could be indicated that the loss function GIOU can fully consider the size of the minimum closure region of the bounding boxes between the prediction box and the real box, and the GIOU has been improved on the loss function of the IOU versus the traditional one. Overall, GIOU could significantly reduce the computational complexity, alongside the complete consideration of the overlapping and non-overlapping regions between the prediction box and the real box. It could be confirmed by the analysis that the proposed model outperforms others in all aspects, with a detection accuracy of 89.5%, which could satisfy the requirements of detection.

To validate the proposed algorithm, the network model was applied to the detection of surface defects in aluminum-plastic blisters.

Compared with the original YOLOv8 model, it was found that the improved YOLOv8 model exhibited higher detection accuracy and recall, a higher probability of detecting blurry objects, alongside overall better performance. Notably, the improved model could enhance the feature extraction ability while retaining the original learning features, which could further enhance the detection effects.

B. Comparative experiment

In this section, the Faster R-CNN, the SSD and the YOLOv5 network model were trained and tested on the same defect sample dataset to further investigate the superiority of the proposed algorithm. The comparison results are shown in TABLE II.

According to TABLE II, the model outperformed other detection models across the aspects of accuracy, recall and mAP@0.5. Compared with the Faster R-CNN algorithm, the accuracy, recall and mAP@0.5 of this algorithm improved by 9.4%, 9.7%, and 12.2%, respectively. Compared with the SSD algorithm, the accuracy, recall and mAP@0.5 of this algorithm improved by 10%, 11.2% and 14.7%, respectively. Additionally, the accuracy, recall and mAP@0.5 of this algorithm improved by 6.8%, 7.3% and 11.4% versus the YOLOv5 algorithm, respectively. In conclusion, the algorithm proposed in this study exhibited better performance than to Faster-RCNN, SSD, and YOLOv5, and YOLOv8, and it could meet the real-time detection requirements.

C. Visual analysis of detection results

With the application of both the optimized algorithm and the YOLOv8 algorithm, the defect detection results of drug aluminum-plastic blister samples were compared to quantitatively evaluate the performance differences between the improved algorithm and the baseline model. As shown in Fig. 5, (a) represents the results from the YOLOv8 algorithm, while (b) shows the results from the proposed algorithm in this research. It could be demonstrated by the results that the improved algorithm outperformed YOLOv8 in both defect detection accuracy and target localization precision. Additionally, YOLOv8 tended to struggle with detecting small defects and low-contrast defects, which would result in missed detections. In contrast, this improved algorithm could effectively identify these subtle defects, alongside the enhancement of overall detection comprehensiveness. Moreover, in terms of bounding box precision, our algorithm could provide more accurate and closely fitting detection boxes, thus reducing the false detection rate.

V. CONCLUSION

This study proposes an improved YOLOv8 real-time detection algorithm for the detection of defects in drug aluminum-plastic blister, which takes into account the characteristics of the drug aluminum-plastic blisters dataset. Compared to other algorithms, this algorithm exhibits several advantages.

Firstly, the Bidirectional Feature Pyramid Network (BiFPN) is introduced into the backbone network of the algorithm, which allows for more effective fusion of information between features of different scales. Secondly, the Group-Shuffle Convolution (GS-Conv) is employed in this method instead of traditional convolutional networks, which could enable more effective feature extraction and expression capabilities the network with smaller model sizes and lower computational effort. Finally, the GIOU loss function is introduced in this study, which takes into account the overlapping and non-overlapping regions between the predicted box and real box, alongside the minimum closure region of their bounding box size, thus contributing to the performance of the algorithm.

It could be revealed by the results that the proposed algorithm outperforms the original algorithm in detecting defects of drug aluminum-plastic blisters, achieving an accuracy of 89.5% and an mAP@0.5 of 82.4%, representing improvements of 3.0% and 3.3%, respectively.

REFERENCES

[1] M. Firouz, K. Mohi-Alden, M. Omid, "A critical review on intelligent and active packaging in the food industry: Research and development," *Food Research International*, vol. 141, pp. 110-113, 2021.

[2] C. Zhuang, Z. Liu, J. Liu, *et al.*, "Digital twin-based quality management method for the assembly process of aerospace products with the Grey-Markov Model and Apriori Algorithm," *Chinese Journal of Mechanical Engineering*, vol. 35, no. 1, p. 105, 2022.

[3] Y. Gao, X. Li, X. Wang, *et al.*, "A review on recent advances in vision-based defect recognition towards industrial intelligence," *Journal of Manufacturing Systems*, vol. 62, pp. 753-766, 2022.

[4] X. Zhan, X. Bu, T. Qin, *et al.*, "X-ray online detection for laser welding T-joint of Al-Li alloy," *Modern Physics Letters B*, vol. 31, no.14, 2017.

[5] A. Bernieri, L. Ferrigno, M. Laracca, *et al.*, "Ultrasonic NDT on aluminum bars: An experimental performance comparison of excitation and processing techniques," *Measurement*, vol. 128, pp. 393-402, 2018.

[6] R. Singh, "Penetrant testing-science direct", *in Applied Welding Engineering*, vol. 3, pp. 339-345, 2020.

[7] R. Singh, "Magnetic particle testing", *in Applied Welding Engineering*, vol. 2, pp. 327-334, 2016.

[8] S. Dong, P. Wang, K. Abbas, "A survey on deep learning and its applications," *Computer Science Review*, vol. 40, 2021.

[9] Y. Gong, M. Liu, X. Wang, *et al.*, "Research on surface defects detection method and system in manufacturing processes based on the fusion of multi-scale features and semantic segmentation for intelligent manufacturing," *Journal of Intelligent & Fuzzy Systems*, vol. 44, no. 4, pp. 6463-6481, 2023.

[10] X. Wang, H. Dai, Z. Huang, *et al.*, "Network Traffic Anomaly Detection Based on DGBi-SA Model," *Engineering Letters*, vol. 33, no. 3, pp. 612-619,2025.

[11] X. Liao, X. Guo, A. Rozi, et al., "PSP-RTMDet: End-to-End Lightweight High-Precision Helmet Detector," *Engineering Letters*, vol. 33, no. 3, pp. 637-649, 2025.

[12] D. Hou, Y. Zhang, J. Ren, "A Lightweight Object Detection Algorithm for Remote Sensing Images," *Engineering Letters*, vol. 33, no.3, pp. 704-711,2025.

[13] R. Girshick, J. Donahue, T. Darrell, *et al*., "Rich feature hierarchies for accurate object detection and semantic segmentation," *Proceedings of the IEEE conference on computer vision and pattern recognition*, pp. 580-587, 2014.

[14] S. Ren, K. He, R. Girshick, *et al*., "Faster R-CNN: Towards real-time object detection with region proposal networks," *IEEE transactions on pattern analysis and machine intelligence*, vol.39, no.6, pp. 1137-1149,2016.

[15] K. He, G. Gkioxari, P. Dollár, *et al*., "Mask r-cnn," *Proceedings of the IEEE international conference on computer vision*, pp. 2961-2969, 2017.

[16] R. Hao, B. Lu, Y. Cheng, *et al*., "A steel surface defect inspection method towards smart industrial monitoring," *Journal of Intelligent Manufacturing*, vol. 32, pp. 1833-1843, 2021.

[17] D. Ma, H. Fang, N. Wang, *et al*., "Automatic detection and counting system for pavement cracks based on PCGAN and YOLO-MF," *IEEE Transactions on Intelligent Transportation Systems*, vol. 23, no. 11, pp. 22166-22178, 2022.

[18] Y. Wang, H. Wang, Z. Xin, "Efficient detection model of steel strip surface defects based on YOLO-V7," *IEEE Access*, vol. 10, pp. 133936–133944.

[19] T. Li, Y. Zhang, Q. Li, T. Zhang, "AB-DLM: An improved deep learning model based on attention mechanism and BiFPN for driver distraction behavior detection," *IEEE Access*, vol. 10, pp. 83138–83151.

[20] Y. Cao, D. Pang, Q. Zhao, *et al*., "Improved yolov8-gd deep learning model for defect detection in electroluminescence images of solar photovoltaic modules," *Engineering Applications of Artificial Intelligence*, vol. 131, 2024.

[21] L. Liu, P. Li, D. Wang, *et al*., "A wind turbine damage detection algorithm designed based on YOLOv8," *Applied Soft Computing*, vol. 154, 2024.

[22] W. Fang, Ye. Wang, "A defect detection method for aluminum-plastic blister drug packaging," *Packaging Engineering*, vol. 40, no. 01, pp. 133-139, 2019.

[23] A. Vijayakumar, S. Vairavasundaram, J. Koilraj, *et al*., "Real-time visual intelligence for defect detection in pharmaceutical packaging," *Scientific Reports*, vol. 14, no.1, p. 18811, 2024.

[24] B. Ma, Z. Hua, Y. Wen, *et al*., "Using an improved lightweight YOLOv8 model for real-time detection of multi-stage apple fruit in complex orchard environments," *Artificial Intelligence in Agriculture*, pp. 1170-1182, 2024.

[25] Q. Chen, X. Jiang, A portable real-time concrete bridge damage detection system[J]. Measurement, 2025,240115536-115536.

[26] J. Redmon, S. Divvala, R. Girshick, *et al*., "You only look once: Unified, real-time object detection," *Proceedings of the IEEE conference on computer vision and pattern recognition*, pp. 779-788, 2016.

[27] M. Liu, Y. Gong, X. Wang, *et al*., "DSN-BR-Based Online Inspection Method and Application for Surface Defects of Pharmaceutical Products in Aluminum-Plastic Blister Packages," *Chinese Journal of Mechanical Engineering*, vol. 37, no. 1, pp. 86, 2024.